

# XANES and XPS Study on Microstructure of Mn-Doped ZnO Films

B. Zhang<sup>1,2</sup>, M. Li<sup>1,2</sup>, J. Z. Wang<sup>1,2</sup>, L. Q. Shi<sup>1,2</sup>, H. S. Cheng<sup>1,2</sup>

<sup>1</sup>Applied Ion Beam Physics Laboratory (Key Laboratory of the Ministry of Education), Institute of Modern Physics, Fudan University, Shanghai, China; <sup>2</sup>Department of Nuclear Science and Technology, Fudan University, Shanghai, China.  
Email: binzhang@fudan.edu.cn

Received January 24<sup>th</sup>, 2013; revised March 27<sup>th</sup>, 2013; accepted April 11<sup>th</sup>, 2013

Copyright © 2013 B. Zhang *et al.* This is an open access article distributed under the Creative Commons Attribution License, which permits unrestricted use, distribution, and reproduction in any medium, provided the original work is properly cited.

## ABSTRACT

Microstructure of ZnO:Mn films with various Mn concentration was investigated with XANES and XPS. The experimental results revealed a substitution of Mn in ZnO and also excluded the existence of Mn oxides or metallic manganese clusters. The substitutional Mn presented a divalent state and all the ZnO:Mn films were n-type. Room temperature ferromagnetism monotonously decreases with the decrease of the electron carrier concentration. The observed ferromagnetism should come from the carrier-mediated exchange.

**Keywords:** ZnO-Based DMS; Mn Substitution; XANES; XPS

## 1. Introduction

Recently, diluted magnetic semiconductors (DMSs) [1-3] have attracted much interest for their potential applications in spintronics. Among them, Mn-doped ZnO is the most favorable candidate because the Mn ion possesses the highest magnetic moment among 3d transition metals and can create a fully polarized stable state due to half-filled 3d bands. There are many reports on room temperature ferromagnetism (RTFM) in the system since the theoretical prediction of RTFM by Dietl *et al.* in 2000 [4]. However, the origin of ferromagnetism (FM) is still unclear. Some studies indicate that FM might come from the precipitates (e.g., clusters and/or a secondary phase) [5-7]. On the other hand, some studies think that FM might originate from exchange interactions between the localized magnetic moment of the substitutional ions on Zn sites and free charge carriers generated by doping [8-10]. Another origin of FM might be defect-mediated coupling of spins [11-13]. In Mn-doped ZnO, the defects are mainly oxygen/zinc vacancies or interstitials. The defect like O vacancies or Zn interstitials might trap an electron, forming an H-like structure. These electrons confined in O vacancies or Zn interstitials would interact with the d-electrons of a Mn atom within their orbits, yielding a bound magnetic polaron (BMP) [14]. The BMPs overlap with each other and hence inducing FM. Recently, FM is also observed in n-type ZnO:Mn films at or above RT,

and the magnetization monotonously depends on the electron carrier concentration [15,16]. The experimental result contradicts the theoretical prediction which requires a high concentration of holes for FM [4,17]. Therefore, to further investigate and clarify the origin of FM, it is very important to investigate microstructure of Mn doped ZnO, especially occupation sites and valent states of Mn atoms.

X-ray absorption near-edge structure (XANES) spectroscopy is a powerful probe for providing a “fingerprint” of chemical states and local electronic structure of incorporated atoms in the host compounds even in a dilute concentration. In particular, the absolute energy position of the edge spectra contains information about the valence state of the absorbing elements. In this paper we employ XANES combining other analysis techniques to investigate the Mn local atomic and electronic structures as well as magnetic interactions in Mn-doped ZnO film.

## 2. Experimental

Mn-doped ZnO films were deposited on (0001) sapphire substrates (99.999%) by radio frequency (RF) magnetron sputtering, with a composite target of ZnO (99.99%) and Mn (99.99%). According to the area ratio of ZnO and Mn, the Mn-doped content could be adjusted. High purity Ar (99.999%) was introduced into the sputtering chamber at the base pressure of  $\leq 6.0 \times 10^{-4}$  Pa. The Ar-

flow rate was 20 SCCM (SCCM denotes cubic centimeter per minute at STP (standard temperature and pressure)). The working pressure was 0.5 Pa, the sputtering power 90 W and the substrate temperature 500°C. Prior to a deposition, a pre-sputtering cleaning was performed for about 20 minutes to eliminate possible contaminants from the target surface.

The Mn K-edge XANES (6.539 keV) spectra were measured at the U7C beamline of National Synchrotron Radiation Laboratory of China. High resolution XPS spectra were detected using a Kratos AXIS Ultra DLD spectrometer with a high resolution of 0.48 eV. The monochromatic Al K $\alpha$  X-ray ( $\lambda = 0.8339$  nm) was used as the incident light. The binding energy scale was calibrated using the C 1s line at 284.8 eV. Electrical properties were carried out at room temperature by Hall effect measurements using a Van der Pauw four-point method. An In electrode was made by soldering indium at four corners of the sample surface. The linear I-V behavior for all samples indicated a good Ohmic contact between In electrode and film layer. The magnetic property at room temperature was measured by the Quantum Design MPMS-XL7 SQUID magnetometer.

### 3. Results and Discussion

To detect Mn cluster and any secondary phases in the ZnO:Mn samples, we have measured Mn K-edge XANES of all the DMS samples and Mn metal. For clarity, **Figure 1** only shows the measured spectra of the Zn<sub>0.89</sub>Mn<sub>0.11</sub>O film and Mn metal. The FEFF 9.0 [18] simulations of Mn oxides (MnO, MnO<sub>2</sub>, Mn<sub>2</sub>O<sub>3</sub>, Mn<sub>3</sub>O<sub>4</sub>) are also shown in **Figure 1**. The spectrum of the DMS sample is quite different from Mn oxides and metallic Mn. The spectrum of MnO has the same features as that of the DMS film in a high energy region (Peak B, C and D), while there is no agreement in the low energy region

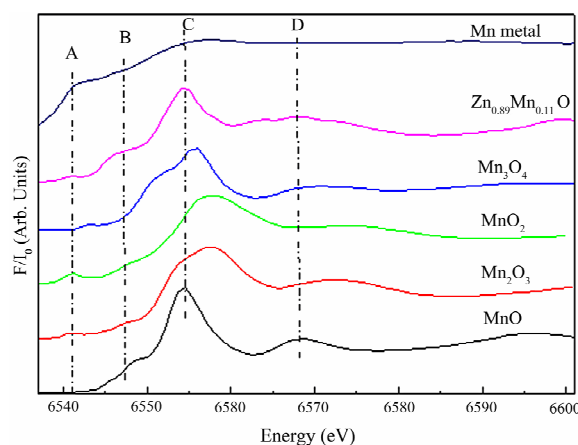


**Figure 1.** Mn K-edge experimental XANES spectra for the Zn<sub>0.89</sub>Mn<sub>0.11</sub>O film and Mn metal, and Mn K-edge calculated XANES spectra for MnO, MnO<sub>2</sub>, Mn<sub>2</sub>O<sub>3</sub> and Mn<sub>3</sub>O<sub>4</sub>.

(Peak A). It implies that there are no Mn oxides or metallic manganese clusters in the films. The same results have been obtained using an extended X-ray absorption fine structure (EXAFS) and synchrotron radiation X-ray diffraction (SR-XRD) [19]. Additionally, the Mn absorption edge position of the DMS samples is close to that of MnO, suggesting the existence of Mn<sup>2+</sup>.

In order to further investigate Mn occupation sites, we have attempted to perform XANES calculations with the FDMNES 2007 code [20] at Mn K-edge for a lot of possible configurations such as the substitutional Mn<sub>Zn</sub>, the interstitial Mn<sub>i</sub>, the Mn<sub>Zn</sub>-Mn<sub>i</sub> dimer, and the Mn<sub>Zn</sub>-O-Mn<sub>Zn</sub>. For the interstitial Mn<sub>i</sub> model, Mn is placed at the void in wurtzite ZnO structure locating at the center of the Zn tetrahedron. The Mn<sub>Zn</sub>-Mn<sub>i</sub> dimer is based on the interstitial structure, where one Zn atom of the Mn-containing tetrahedron is substituted by a Mn atom. For the Mn<sub>Zn</sub>-O-Mn<sub>Zn</sub>, two substitutional Mn atoms on Zn sites are separated by an O atom. All XANES functions are calculated within a sphere of 6 Å radius, whose center is the absorber atom Mn. **Figure 2** shows the spectra of the DMS samples and the calculated spectra from the above-mentioned models. Obviously, the spectra of the DMS samples are different from that of the interstitial Mn<sub>i</sub>, which means that Mn could not exist at the interstitial site. We also explore the clustering tendency of the Mn atoms in ZnO. From the obvious difference between the spectra of the Mn<sub>Zn</sub>-Mn<sub>i</sub> dimer, the Mn<sub>Zn</sub>-O-Mn<sub>Zn</sub> and the DMS samples, we can exclude the phenomena. In the XANES spectra of the DMS samples, there are four characteristic peaks A (6541 eV), B (6546 eV), C (6555 eV) and D (6567 eV). The preedge peak A can be interpreted as the transition of Mn 1s core electron to the unoccupied Mn 3d and O 2p hybridized states. In the substitutional model, “Mn<sub>Zn</sub>” represent the model of no op-

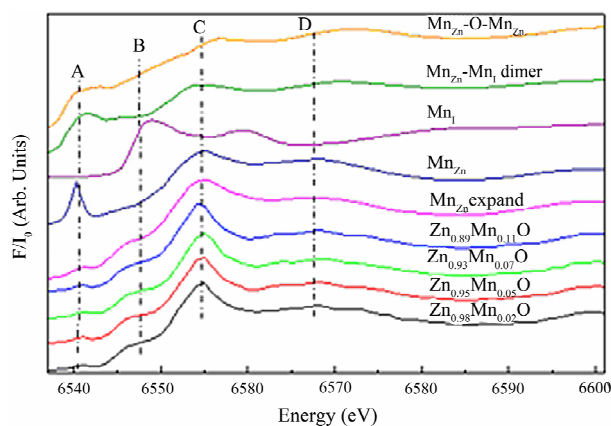


**Figure 2.** Mn K-edge experimental XANES spectra for the Zn<sub>1-x</sub>Mn<sub>x</sub>O films and Mn K-edge calculated XANES spectra for different Mn occupation sites in wurtzite ZnO lattice: substitutional Mn<sub>Zn</sub>, interstitial Mn<sub>i</sub>, Mn<sub>Zn</sub>-Mn<sub>i</sub> dimer, and Mn<sub>Zn</sub>-O-Mn<sub>Zn</sub>.

timizing the geometry of the studied configurations, *i.e.*, the bond lengths of  $\text{Mn}_{\text{Zn}}\text{-O}$  and  $\text{Mn}_{\text{Zn}}\text{-Zn}$  is 1.97 and 3.20 Å, respectively, while “ $\text{Mn}_{\text{Zn}}$  expand” represent the model in which the bond lengths of  $\text{Mn}_{\text{Zn}}\text{-O}$  and  $\text{Mn}_{\text{Zn}}\text{-Zn}$  is expanded to 2.03 and 3.28 Å, respectively. In the  $\text{Mn}_{\text{Zn}}$  model, A, C and D peaks can be well reproduced except the B peak. On the other hand, the height of the Peak A in the  $\text{Mn}_{\text{Zn}}$  model is much larger than that in the DMS samples. However, in the  $\text{Mn}_{\text{Zn}}$  expand model, four characteristic peaks can be well reproduced and the calculated spectrum resembles those of the DMS samples. It implies that Mn atoms are incorporated into the ZnO crystal lattice by the substitution on Zn sites, accompanying with an expansion of the  $\text{Mn}_{\text{Zn}}\text{-O}$  and  $\text{Mn}_{\text{Zn}}\text{-Zn}$  bond lengths due to the larger atomic radius of Mn compared with Zn. The same results have been observed by an extended X-ray absorption fine structure (EXAFS) [19].

The valent state of Mn in the DMS films is detected by high resolution XPS. In **Figure 3**, the Mn  $2p_{3/2}$  peak for the DMS samples is located at 640.73 eV, which is very close to  $\text{Mn}^{2+}$  in MnO (Mn  $2p_{3/2}$ : 640.7 eV) according to the XPS handbook. It well agrees with those reported in the literature, indicating a divalent state of the Mn ions in ZnO:Mn films [21,22]. Moreover, from the XPS handbook we also know that the Mn  $2p_{3/2}$  peaks for metallic Mn,  $\text{Mn}_3\text{O}_4$ ,  $\text{Mn}_2\text{O}_3$  and  $\text{MnO}_2$  are located at 639, 641.2, 641.6 and 642.2 eV, respectively. So we can exclude the existence of Mn oxides or metallic manganese clusters in the films, in good agreement with the XANES analysis.

**Figure 4** shows the magnetization curves at room temperature. These magnetization curves are obtained with the applied field parallel to the plane of the sample. The diamagnetic background of ZnO and sapphire substrate are subtracted. The hysteresis loops show the clear ferromagnetic behavior of these Mn-doped ZnO films at room temperature. From **Figure 4**, the saturation mag-

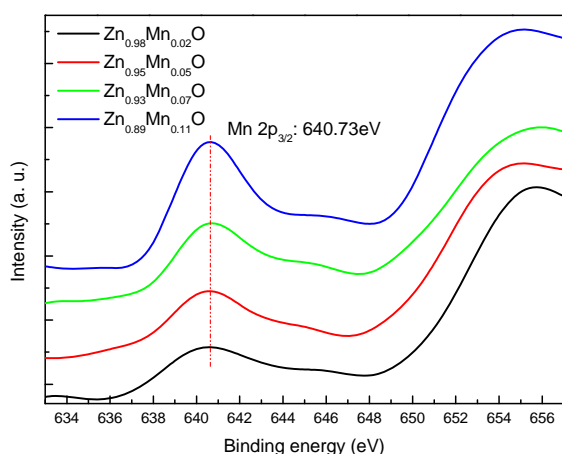


**Figure 3.** The high resolution XPS Mn-2p spectra for the  $\text{Zn}_{1-x}\text{Mn}_x\text{O}$  films.

netic moment ( $M_s$ ) first decreases as Mn content increases from 2 to 7 at%, and then remain at Mn content from 7 to 11 at%.

Hall effect was used to detect the carrier type and concentration of these Mn-doped ZnO films. The results show that all the Mn-doped ZnO films are n-type. For the 2 at% Mn doping, the carrier concentration ( $n$ ) and the saturation magnetic moment ( $M_s$ ) are  $2.86 \times 10^{18} \text{ cm}^{-3}$  and  $0.083 \mu_B/\text{Mn}$ , respectively, while for 5 at%,  $n$  and  $M_s$  are  $3 \times 10^{17} \text{ cm}^{-3}$  and  $0.016 \mu_B/\text{Mn}$ , respectively. The values of  $n$  and  $M_s$  ( $n: 1 \times 10^{17} \text{ cm}^{-3}$ ,  $M_s: 0.015 \mu_B/\text{Mn}$ ) for 7 at% are the same as that for 11 at%. From **Figure 5**, ferromagnetism monotonously decreases with the decrease of the electron carrier concentration, in good agreement with the results in Refs. [15,16]. According to the Zener model [4], which explains the exchange interaction between the magnetic impurity atoms in the DMS as mediated by free charge carrier, the increase in charge carrier concentration can enhance the magnetic or-

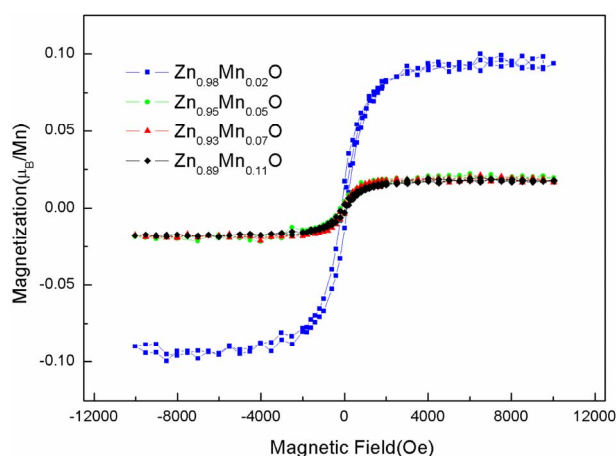


**Figure 4.** Hysteresis loops for the  $\text{Zn}_{1-x}\text{Mn}_x\text{O}$  films.

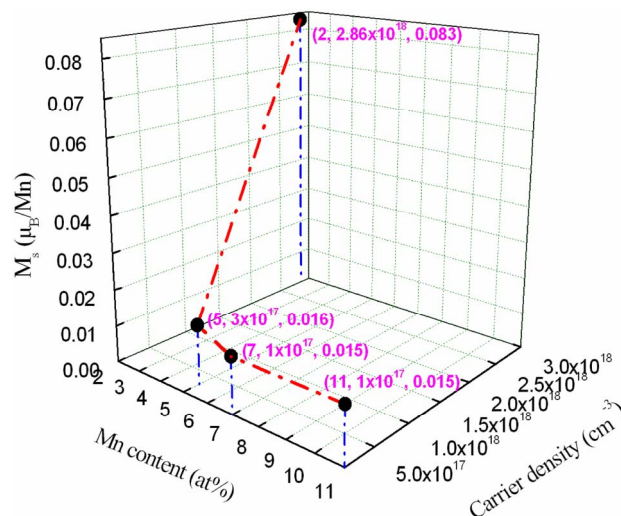


**Figure 5.**  $M_s$  as a function between Mn concentration and carrier density for the  $\text{Zn}_{1-x}\text{Mn}_x\text{O}$  films.

dering. Therefore, we deduce that our observed ferromagnetism should come from the carrier-mediated exchange.

#### 4. Conclusion

ZnO films doped with different Mn concentration were deposited on sapphire substrates by RF magnetron sputtering. The measurements revealed a substitution of Mn in ZnO and also excluded the existence of Mn oxides or metallic manganese clusters. The substitutional Mn presented a divalent state and all the ZnO:Mn films were n-type. Room temperature ferromagnetism monotonously decreases with the decrease of the electron carrier concentration. The observed ferromagnetism should come from the carrier-mediated exchange.

#### 5. Acknowledgements

This work is supported by the National Natural Science Foundation of China (Grant Nos. 10775033 and 11075038). The authors would like to thank the U7C beam line of National Synchrotron Radiation Laboratory of China for providing the beam time.

#### REFERENCES

- [1] B. Zhang, Q. H. Li, L. Q. Shi, H. S. Cheng and J. Z. Wang, "Room Temperature Ferromagnetism of Fe-Implanted ZnO Film," *Journal of Vacuum Science & Technology A*, Vol. 26, No. 6, 2008, pp. 1469-1473. [doi:10.1116/1.2990855](https://doi.org/10.1116/1.2990855)
- [2] B. Zhang, L. Q. Shi, C. C. Chen and D. G. Zhao, "PIXE Analysis of Fe Content in Fe-Implanted GaN Film," *Nuclear Instruments and Methods in Physics Research Section B*, Vol. 252, No. 2, 2006, pp. 225-229. [doi:10.1016/j.nimb.2006.09.007](https://doi.org/10.1016/j.nimb.2006.09.007)
- [3] X. F. Wang, J. B. Xu, W. Y. Cheng, J. An and N. Ke, "Aggregation-Based Growth and Magnetic Properties of Inhomogeneous Cu-Doped ZnO Nanocrystals," *Applied Physics Letters*, Vol. 90, No. 21, 2007, Article ID: 212502. [doi:10.1063/1.2741408](https://doi.org/10.1063/1.2741408)
- [4] T. Dietl, H. Ohno, F. Matsukura, J. Cibert and D. Ferrand, "Zener Model Description of Ferromagnetism in Zinc-Blende Magnetic Semiconductors," *Science*, Vol. 287, No. 5455, 2000, pp. 1019-1022. [doi:10.1126/science.287.5455.1019](https://doi.org/10.1126/science.287.5455.1019)
- [5] A. C. Tuan, J. D. Bryan, A. B. Pakhomov, V. Shutthanandan, S. Thevuthasan, D. E. McCready, D. Gaspar, M. H. Engelhard, J. W. Rogers Jr., K. Krishnan, D. R. Gamelin and S. A. Chambers, "Epitaxial Growth and Properties of Cobalt-Doped ZnO on  $\alpha$ -Al<sub>2</sub>O<sub>3</sub> Single-Crystal Substrates," *Physical Review B*, Vol. 70, No. 5, 2004, Article ID: 054424. [doi:10.1103/PhysRevB.70.054424](https://doi.org/10.1103/PhysRevB.70.054424)
- [6] X. Z. Li, J. Zhang and D. J. Sellmyer, "Structural Study of Mn-Doped ZnO Films by TEM," *Solid State Communications*, Vol. 141, No. 7, 2007, pp. 398-401. [doi:10.1016/j.ssc.2006.11.022](https://doi.org/10.1016/j.ssc.2006.11.022)
- [7] K. Potzger, S. Q. Zhou, H. Reuther, A. Mücklich, F. Eichhorn, N. Schell, W. Skorupa, M. Helm, J. Fassbender, T. Herrmannsdörfer and T. P. Papageorgiou, "Fe Implanted Ferromagnetic ZnO," *Applied Physics Letters*, Vol. 88, No. 5, 2006, Article ID: 052508. [doi:10.1063/1.2169912](https://doi.org/10.1063/1.2169912)
- [8] C. Yang, B. Zhang, J. Z. Wang, L. Q. Shi, H. S. Cheng, T. Y. Yang, W. Wen and F. C. Hu, "Microstructure and Room Temperature Ferromagnetism of Cu-Doped ZnO Films," *Nuclear Instruments and Methods in Physics*, Vol. 283, 2012, pp. 24-28. [doi:10.1016/j.nimb.2012.04.007](https://doi.org/10.1016/j.nimb.2012.04.007)
- [9] C. Yang, B. Zhang, J. Z. Wang, L. Q. Shi, H. S. Cheng, T. Y. Yang, W. Wen and F. C. Hu, "EXAFS and SR-XRD Study on Cu Occupation Sites in Zn<sub>1-x</sub>Cu<sub>x</sub>O Diluted Magnetic Semiconductors," *Nuclear Science and Techniques*, Vol. 23, 2012, pp. 65-69.
- [10] X. J. Liu, X. Y. Zhu, C. Song, F. Zeng and F. Pan, "Intrinsic and Extrinsic Origins of Room Temperature Ferromagnetism in Ni-Doped ZnO Films," *Journal of Physics D: Applied Physics*, Vol. 42, 2009, Article ID: 035004. [doi:10.1088/0022-3727/42/3/035004](https://doi.org/10.1088/0022-3727/42/3/035004)
- [11] D. Gao, Z. Zhang, J. Fu, Y. Xu, J. Qi and D. Xue, "Room Temperature Ferromagnetism of Pure ZnO Nanoparticles," *Journal of Applied Physics*, Vol. 105, No. 11, 2009, Article ID: 113928. [doi:10.1063/1.3143103](https://doi.org/10.1063/1.3143103)
- [12] S. Banerjee, M. Mandal, N. Gayathri and M. Sardar, "Enhancement of Ferromagnetism upon Thermal Annealing in Pure ZnO," *Applied Physics Letters*, Vol. 91, No. 18, 2007, Article ID: 182501. [doi:10.1063/1.2804081](https://doi.org/10.1063/1.2804081)
- [13] X. G. Chen, Y. B. Yang, R. Wu, R. Liu, X. D. Kong, L. Han, Y. C. Yang and J. B. Yang, "Room Temperature Magnetic Properties of ZnO Nanostructured Films," *Physica B*, Vol. 406, No. 6, 2011, pp. 1341-1344. [doi:10.1016/j.physb.2011.01.030](https://doi.org/10.1016/j.physb.2011.01.030)
- [14] J. M. D. Coey, M. Venkatesan and C. B. Fitzgerald, "Donor Impurity Band Exchange in Dilute Ferromagnetic Oxides," *Nature Materials*, Vol. 4, No. 2, 2005, pp. 173-179. [doi:10.1038/nmat1310](https://doi.org/10.1038/nmat1310)
- [15] Z. Yang, J. L. Liu, M. Biasini and W. P. Beyermann, "Electron Concentration Dependent Magnetization and Magnetic Anisotropy in ZnO:Mn Thin Films," *Applied Physics Letters*, Vol. 92, No. 4, 2008, Article ID: 042111. [doi:10.1063/1.2838753](https://doi.org/10.1063/1.2838753)
- [16] M. Ivill, S. J. Pearton, Y. W. Heo, J. Kelly, A. F. Hebard and D. P. Norton, "Magnetization Dependence on Carrier Doping in Epitaxial ZnO Thin Films Co-Doped with Mn and P," *Journal of Applied Physics*, Vol. 101, No. 12, 2007, Article ID: 123909. [doi:10.1063/1.2739302](https://doi.org/10.1063/1.2739302)
- [17] K. Sato and H. Katayama-Yoshida, "Material Design for Transparent Ferromagnets with ZnO-Based Magnetic Semiconductors," *Japanese Journal of Applied Physics Part 2*, Vol. 39, 2000, pp. L555-L558. [doi:10.1143/JJAP.39.L555](https://doi.org/10.1143/JJAP.39.L555)
- [18] A. L. Ankudinov, B. Ravel, J. J. Rehr and S. D. Conradson, "Real-Space Multiple-Scattering Calculation and Interpretation of x-Ray-Absorption Near-Edge Structure," *Physical Review B*, Vol. 58, No. 12, 1998, pp. 7565-7576. [doi:10.1103/PhysRevB.58.7565](https://doi.org/10.1103/PhysRevB.58.7565)
- [19] M. Li, B. Zhang, J. Z. Wang, L. Q. Shi, H. S. Cheng, Y. Z. Wang, H. Y. Lv, T. Y. Yang, W. Wen and F. C. Hu,

- “EXAFS and SR-XRD Study on Mn Occupations in  $Zn_{1-x}Mn_xO$  Diluted Magnetic Semiconductors,” *Nuclear Instruments and Methods in Physics Research Section B*, Vol. 269, No. 21, 2011, pp. 2610-2613.  
[doi:10.1016/j.nimb.2011.07.094](https://doi.org/10.1016/j.nimb.2011.07.094)
- [20] Y. Joly, “X-Ray Absorption Near-Edge Structure Calculations beyond the Muffin-Tin Approximation,” *Physical Review B*, Vol. 63, No. 12, 2001, Article ID: 125120.  
[doi:10.1103/PhysRevB.63.125120](https://doi.org/10.1103/PhysRevB.63.125120)
- [21] H. Y. Xu, Y. C. Liu, C. S. Xu, Y. X. Liu, C. L. Shao and R. Mu, “Room-Temperature Ferromagnetism in (Mn, N)-Codoped ZnO Thin Films Prepared by Reactive Magnetron Cosputtering,” *Applied Physics Letters*, Vol. 88, No. 24, 2006, Article ID: 242502. [doi:10.1063/1.2213929](https://doi.org/10.1063/1.2213929)
- [22] Z. B. Gu, M. H. Lu, J. Wang, D. Wu, S. T. Zhang, X. K. Meng, Y. Y. Zhu, S. N. Zhu, Y. F. Chen and X. Q. Pan, “Structure, Optical, and Magnetic Properties of Sputtered Manganese and Nitrogen-Codoped ZnO Films,” *Applied Physics Letters*, Vol. 88, No. 8, 2006, Article ID: 082111.  
[doi:10.1063/1.2178466](https://doi.org/10.1063/1.2178466)